Biochemical and Biophysical Research Communications 459 (2015) 196–200

Contents lists available at ScienceDirect

Biochemical and Biophysical Research Communications

journal homepage: www.elsevier.com/locate/ybbrc

UNC-51-like kinase 1 blocks S6k1 phosphorylation contributes to neurodegeneration in Parkinson's disease model *in vitro*

Yongle Li [a, *, 1], Jun Zhang [b, 1], Chunxiang Yang [b]

[a] Graduate School of Tianjin Medical University, 22 Qixiangtai Road, Tianjin 300070, China
[b] Department of Nerve Internal Medicine, Jingmen No.2 People's Hospital, Xiangshan Road, Jingmen 448000, China

ARTICLE INFO

Article history:
Received 27 January 2015
Available online 11 February 2015

Keywords:
Ribosomal protein s6 kinase 1
UNC-51-like kinase 1
Phosphorylation
Parkinson's disease

ABSTRACT

Objective: This study was aim to determine the role and underling mechanism of ribosomal protein S6 kinases 1 (S6k1) phosphorylation in Parkinson's disease (PD).
Methods: The dopaminergic neuron MN9D was employed and 1-methyl-4-phenylpyridium (MPP) iodide (MPP^+) was used to generate PD model *in vitro*. The S6k1 phosphorylation and UNC-51-like kinase 1 (ULK1) protein levels were analyzed by western blot. The ULK1 mRNA level was evaluated by Real-time RT-PCR. The S6k1 threonine 389 (T389) site-directed mutagenesis, the phosphodeficit T389A (threonine to alanine) and the phosphomimetic T389D (threonine to aspartate) were generated to examine the phosphorylation site of S6k1.
Results: An increase in the ULK1 mRNA and protein levels were detected in the MPP^+-treated MN9D cells compared to control. ULK1 knockdown increased neuronal cell viability, and enhanced S6k1 phosphorylation. Further investigation demonstrated ULK1 knockdown promoted the S6k1 T389 phosphorylation in particular. T389A enhanced the viability of MPP iodide-treated MN9D, whereas T389D decreased the cell viability.
Conclusion: ULK1 acts to inhibit S6k1 phosphorylation at T389, leading to MN9D viability reduction under MPP^+ treatment. These results provide evidence for a novel mechanism by which the ULK1 inhibit S6k1 T389 phosphorylation contributes to neurodegeneration in MPP^+ treated-MN9D, and suggests a new therapeutic strategy for PD.

1. Introduction

Parkinson's disease (PD) is a chronic central nervous system degenerative disorder and the pathological change is dopaminergic (DA) neurons selective loss in the substantia nigra pars compacta (SNc) [1]. The brain requires sufficient DA to control muscle movement, and loss of DA neurons triggers a DA deficiency that produces a variety of movement disorders. However, the molecular mechanism underlying the loss of DA neurons has not yet been elucidated.

Ribosomal protein S6 kinases 1 (S6k1, also named p70 S6K) is a signal transduction regulator which implicated in mammalian life span [2], as well as age-related pathologies such as insulin resistance [3] and neuronal death in PD [4]. It is well known that the activity of S6k1 is tightly coupled to its phosphorylation status. Phosphorylation at threonine 389 (T389) 389 is a critical event in S6k1 activation [5]. Rapamycin complex 1 (mTORC1) is known to phosphorylate S6k1 at T389 and thereby activate S6k1 [6]. It has been reported that inhibition of the mTORC1/S6K1 pathway by rotenone contributes to neuron apoptosis [7].

Previous work demonstrated that UNC-51-like kinase 1 (ULK1), a serine/threonine kinase, induces phosphorylation the mTORC1 component raptor, play an important role in mTORC1 inhibition [8]. And recent research demonstrated that both sustained activation and prolonged inactivation of mTOR signaling contributing to AD and PD progression [9,10]. ULK1 negatively regulates S6k1 activity in drosophila and mammalian cells, suggesting possible crosstalk between ULK1 and the mTORC1 pathway [11]. ULK1 induce mTORC1 inhibition, which blocks S6K1 phosphorylation at T389 [12]. However, whether ULK1 regulate the mTORC1/S6K1 pathway in PD is poorly understood.

In the present report, we show that ULK1 blocks S6K1 phosphorylation at T389 contributes to neurodegeneration in 1-methyl-4-phenylpyridium (MPP) iodide (MPP^+)-induced PD cell model, suggesting a new therapeutic strategy to PD.

* Corresponding author. Fax: +86 029 86673458.
E-mail address: yongle_li@126.com (Y. Li).
[1] These two authors contributed equally to this work.

http://dx.doi.org/10.1016/j.bbrc.2015.02.008
0006-291X/

2. Materials and methods

2.1. Cell culture and MPP iodide treatment

The MN9D cells was purchase from ATCC, and the cells were cultured in Dulbecco's modified Eagle's medium with 10% fetal bovine serum in a humidified 5% CO_2 atmosphere at 37 °C. After transfection, the cells were treated with 50 or 100 μM MPP^+ (Sigma, St. Louis, MO, USA) for 24 h to mimic the MPTP-induced *in vivo* model according to previous reports [13].

2.2. Tyrosine hydroxylase immunofluorescence staining

MN9D were incubated with 50 μM or 100 μM MPP^+ for 24 h and then harvested for immunofluorescence staining. Cells attached to coverslips were fixed with 4% paraform for 30 min at 25 °C, rinsed 3 times with PBS and blocked in 1% BSA containing 0.3% Triton X-100. Cells were then rested for 1 h at room temperature. Following this, cells were incubated overnight at 4 °C with rabbit anti tyrosine hydroxylase (1:2000) (Abcam, Cambridge, UK). After rinsed with PBS for 3 times, the coverslips were incubated with Alexa Fluor-488 donkey anti-mouse IgG (1:400) (Invitrogen, Carlsbad, CA, USA) for 2 h at 25 °C. Then, the coverslips were rinsed 3 times with PBS. MN9D were visualized and captured using a fluorescence microscope at 488 nm excitation and 519 nm emission with a camera attachment. The axon length of tyrosine hydroxylase-positive cells were measured using an Image-Pro Plus 6.0 software.

2.3. Real-time RT-PCR

MN9D were exposed to MPP^+ (50 or 100 μM) for 24 h. Then cells were harvested and subjected to subcellular fractionation for RNA isolation. Total RNA from MN9D were isolated using TRIzol reagent (Invitrogen, Carlsbad, CA, USA), and then converted to cDNA using the PrimeScript® RT reagent kit (Takara, Dalian, China) with oligo-dT primers. ULK1 primers were: 5′-AAGGGAAGTGCCAGTGAGG-3′ (sense), 5′-TGTCTGCCTGGTCCGTGA-3′ (anti-sense). β-actin was used as the normalization control for ULK1 gene. Real-time RT-PCR was performed in an Rotor-Gene RG-3000 Real-Time Thermal Cycler (Corbett Research, Australia.).

2.4. Western blotting

The proteins were extracted from the cells using RIPA lysis buffer (Beyotime, Nantong, China). For western blot, equal amounts of proteins were separated on SDS-PAGE and blotted onto a pre-wet nitrocellulose membrane (GE healthcare, Germany), followed by blocking of membranes in 10% defatted milk in PBS at 4 °C overnight, the membranes were then probed with different primary antibodies. The primary antibodies were as following: mouse anti-p-Sk61, anti-p-Sk61 serine (S411), anti-p-Sk61 threonine 421 (T421)/serine 424 (S424), anti-p-Sk61 T389, anti-ULK1, anti-β-actin monoclonal antibody (Santa Cruz, CA, USA). After extensive washing with TBST buffer, the membranes were incubated for 1 h at 25 °C with HRP-conjugated secondary antibody (KangChen Bio-tech, Shanghai, China). Specific bands were visualized by ECL reagent (Beyotime, Nantong, China). The luminescence was scanned using a Typhoon scanner (Amersham Biosciences, Piscataway, NJ, USA).

2.5. Cell viability

Cell viability were measured using the MTS assay (CellTiter96 AQ, Promega, Madison, WI) according to the previous study [14]. Briefly, cells were grown on collagen-coated 96 well plates, and

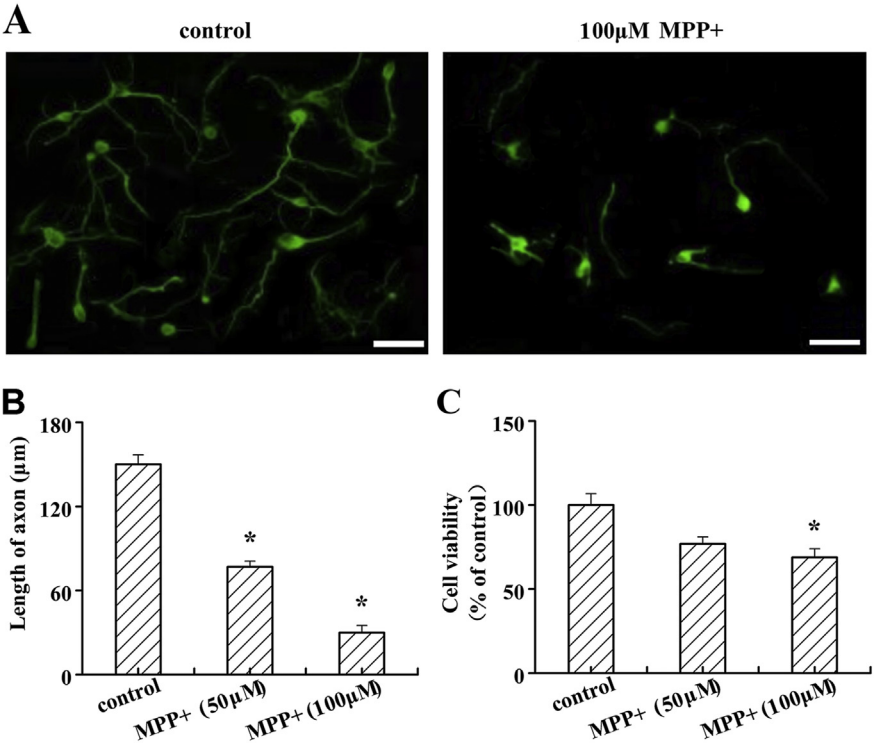

Fig. 1. MPP iodide (MPP^+)-induced neurotoxicity in MN9D. After treated with 100 μM MPP^+ for 24 h, the cells were labeled with rabbit anti tyrosine hydroxylase antibody and detected using Alexa Fluor-488 donkey anti-mouse IgG antibody, scale bar indicates 50 μm (A). The axan length (B) and cell viability (C) in MN9D after exposed to 50 or 100 μM MPP^+ iodide for 24 h. Each bar represents mean ± SD. $^*P < 0.05$, compare to control group.

then 20 μl of reagent was administered to each well for 3 h at 37 °C and in a 5% CO_2 atmosphere. Then the wells were evaluated for colorimetric absorption with a spectrophotometer (Beckman, USA).

2.6. Site-directed mutagenesis

The cDNA of mouse S6k1 (NM_001114334.1) was subcloned into a pCMV-3Tag-3 mammalian expression vector to produce a vector (Flag-S6k1-WT) encoding full-length mouse S6k1 protein tagged with Flag epitope. Site-directed mutagenesis was subsequently performed to generate 2 constructs in which T389 was replaced by either alanine (Flag-S6k1-T389A) or aspartate (Flag-S6k1-T389D). Transient transfection was performed in MN9D with effectene transfection reagent (QIAGEN, Germany), and overexpression was confirmed by western blot using the anti-Flag antibody.

2.7. Statistical analysis

Data were presented as mean ± SE. Statistical analyses were performed using SPSS19.0 software (SPSS, Chicago, IL). Statistical significance was assessed by one-way ANOVA (Dunnett's test). A P value <0.05 was considered as statistically significant.

3. Results

3.1. MPP iodide induces cell damage in MN9D

After MN9D were exposed to MPP^+ (50 or 100 μM) for 24 h, the cells were harvested for tyrosine hydroxylase immunofluorescence staining, axon length qualification and cell viability determination. Treating MN9D with 100 μM MPP^+ for 24 h resulted in typical morphological changes, such as axon shortening and cell body shrinkage, as signs of neurodegeneration (Fig. 1A). Furthermore, the axon length was decreased with the increasing MPP iodide concentrations (Fig. 1B). Both 50 μM and 100 μM MPP^+ treatments significantly decreased the MN9D viability. Approximately 50% cell loss was observed after treatment with MPP^+ for 24 h at a concentration of 100 μM (Fig. 1C).

3.2. MPP iodide inhibits S6k1 phosphorylation in MN9D

S6k1 is implicated in neuronal cell death in *in vitro* models of PD [4]. In order to elucidate whether MPP^+ induced changes of S6k1 phosphorylation in MN9D, we determined the phosphorylation levels of S6k1 by western blot. As shown in Fig. 2A, after MPP^+ treatment, a dose-dependent decrease in S6k1 phosphorylation

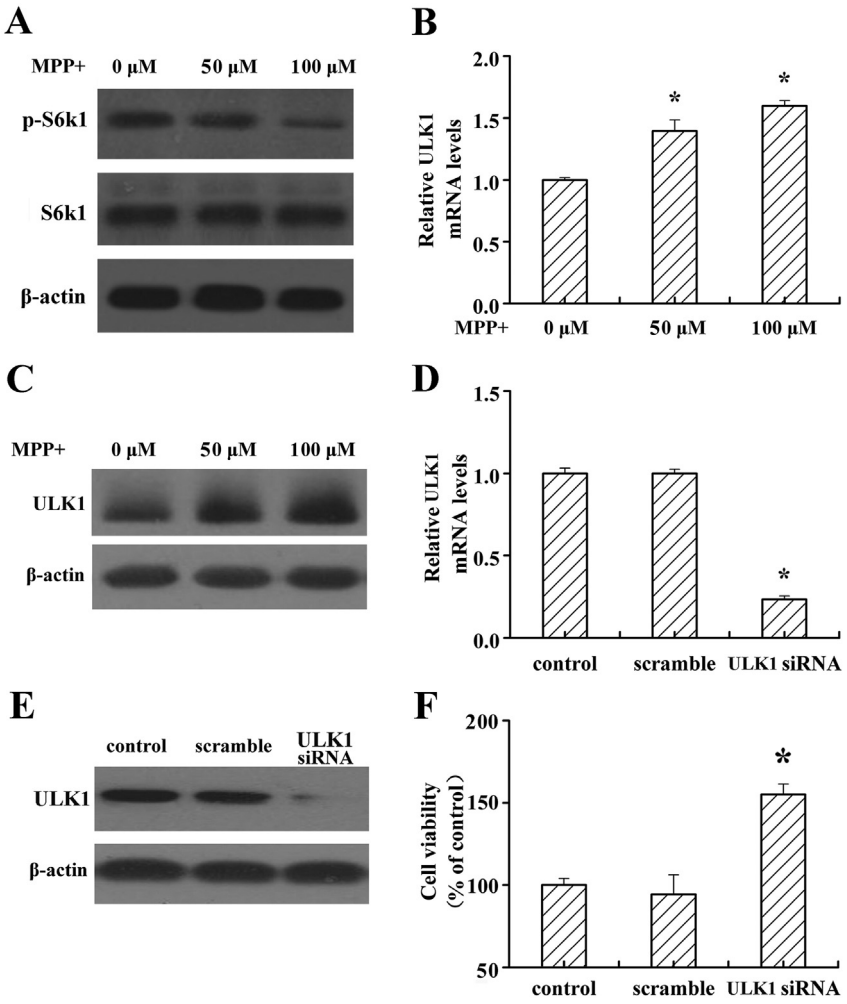

Fig. 2. MPP iodide (MPP^+) inhibits S6K1 phosphorylation and induces ULK1 expression in MN9D; ULK1 knocked down promotes MN9D viability after MPP iodide (MPP+) treatment. The phosphorylation levels of S6K1 (A), the mRNA (B) and protein (C) levels of ULK1 in MN9D after exposed to 50 or 100 μM MPP^+ for 24 h. The ULK1 protein (D) and mRNA (E) levels, and the cell viabilities of MPP^+-treated MN9D (F) after ULK1 knocked down. Data bars represent the means ± SD. $^*P < 0.05$, compare to control group.

levels was observed in the 50 μM and 100 μM MPP + treated groups compared to the 0 μM MPP^+ treated groups.

3.3. ULK1 mRNA and protein levels in MPP^+-treated MN9D cells

previous report shown ULK1 was involved in the progression of neurodegeneration in PD [15], in order to elucidate whether ULK1 involved in MPP^+-induced toxicity in MN9D, we determined its mRNA and protein expression levels by real-time RT-PCR and western blot. As shown in Fig. 2B, ULK1 mRNA levels were significantly increased in the 50 μM and the 100 μM MPP^+ treated group ($P < 0.05$); a dose-dependent increase in ULK1 protein level was also observed in the MPP^+ treated groups compared to the control (Fig. 2C).

3.4. Cell viability after ULK1 knockdown

In order to address the effect of endogenous ULK1 in MPP^+ treated MN9D, ULK1 specific siRNA was used to knock down the ULK1 gene and the cell viability under MPP^+ treatment was measured. Scrambled siRNA had no effect on the mRNA and protein levels of ULK1 in MN9D, and it also had no effect on the cell viability under MPP^+ treatment. In contrast, ULK1 siRNA significantly decreased the protein and mRNA levels of ULK1 (Fig. 2D, E), and produced about 20% greater cells survival with MPP^+ treatment than in the control group. These results demonstrated that ULK1 was implicated in MPP^+-induced MN9D degeneration (Fig. 2F).

3.5. ULK1 inhibits S6k1 phosphorylation at T389

Previous research has indicated that ULK1 inhibit S6K1 phosphorylation specifically at T389 in mammalian cells [16]. In order to investigate whether ULK1 inhibit S6k1 phosphorylation in MPP^+-induced MN9D, the phosphorylation level of S6k1 was determined after ULK1 knockdown. As the results shown in Fig. 3A, knockdown of ULK1 increased the phosphorylation level of S6k1. Further experiments demonstrated that ULK1 siRNA strongly enhanced S6K1 phosphorylation at T389, whereas T421/S424 and S411 phosphorylation remained unaffected (Fig. 3B).

3.6. Cell viability is associated with increased phosphorylation of S6k1 at T389

In order to better understand the function of S6k1 phosphorylation in the MPP^+-induced death of MN9D, we generated S6k1 T389 site-directed mutagenesis, the phosphodeficit T389A (serine to alanine) and the phosphomimetic T389D (serine to aspartate). Transgenic S6k1 T389A and S6k1 T389D expression were confirmed by western blot using anti-Flag antibody. The results showed that substitution of T389 with alanine in Sk61 significantly blocked S6k1 phosphorylation at T389, whereas with aspartate enhanced S6k1 phosphorylation at T389 (Fig. 3C). As the results of cell viability shown in Fig. 3D, compared with S6k1-WT and control, T389A exhibited a significantly increased in cell viability (Fig. 3D), whereas T389D possessed an obvious decrease in cell viability. These data clearly demonstrated that inhibiting the phosphorylation of S6k1 at T389 enhanced the MPP^+-induced neurotoxin in MN9D.

4. Discussion

PD is a neurodegenerative disorder causing severe motor and language disabilities in elder people [17]. Numerous investigations have focus on the underlying mechanism involved in the progression of PD in recent decades; however, neither the cause nor mechanisms underlying PD have been clarified. The MPTP model replicates most of the biochemical and pathological alterations in PD, including the loss of the DA neurons of the SNc in several mammalian species, and is considered as a superior experimental model for human PD molecular mechanisms investigation [18]. The mouse DA neurons MN9D was used to model PD *in vitro*

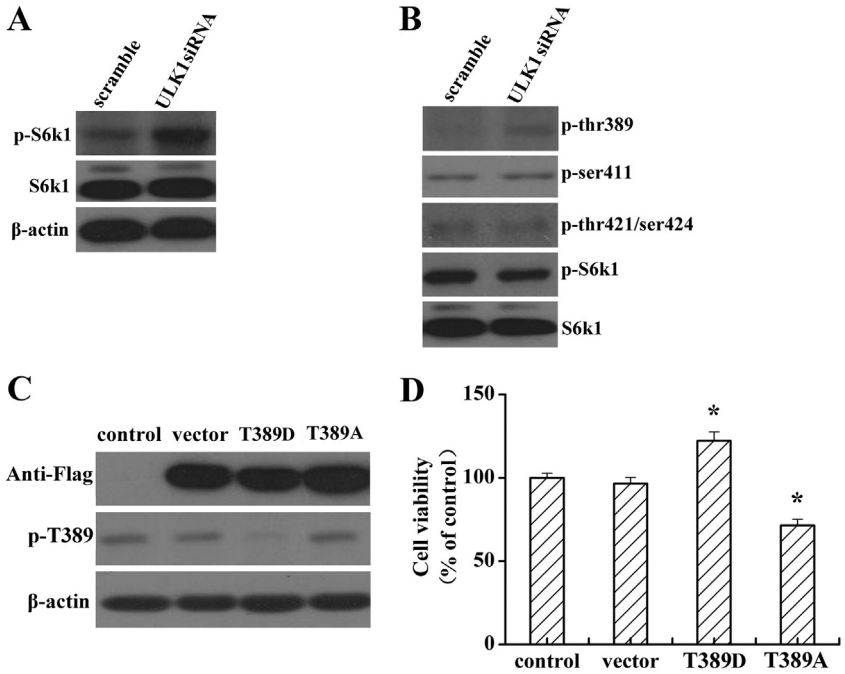

Fig. 3. ULK1 knocked down promotes S6K1 phosphorylation in MN9D; the cell viabilities in S6K1 thr389 site-direct mutations. The total S6K1 (A) and S6K1 phosphorylated at thr389 (p-thr389), ser411 (p-ser411), and thr-421/ser-424 (p-thr421/ser424) (B). MN9D were transiently transfected with wild type (WT), T389A, or T389D Flag-S6K1. Anti-Flag and anti-p-thr389 antibodies were subjected to western blot analysis (C). Cell viabilities were detected in wild type (WT), T389A, or T389D S6K1 transfected MN9D (D). Data bars represent the means ± SD. *$P < 0.05$, compare to control group.

without the influence of the other cell types present in the SNc and surrounding brain regions, and MPP^+ was used to generate a PD model *in vitro*. In this study, we found that MPP^+ treatment induced neurodegeneration, manifest as MN9D death and axon length shrink, indicating the PD cell model was successfully generated.

S6k1 is a major substrate of mTORC1, the mTORC1/S6K1 signal regulates diverse cellular processes including protein synthesis, cell growth, and survival [19]. Previous research reported that inhibition of the mTORC1/S6K1 pathway contributes to neuron apoptosis [7]. The activity of S6k1 depends on its phosphorylation status. In order to elucidate whether MPP^+ treatment induced changes in S6K1 activity, we determined S6k1 phosphorylation after MPP^+ treatment. The results showed that MPP^+ treatment induced S6k1 phosphorylation inhibition in MN9D, indicating S6k1 was involved in the preprocessed of PD.

Our result demonstrated that ULK1 expression was elevated in MPP^+ treated-MN9D cells in a dose-dependent effect, this phenomenon indicated that ULK1 might play a prominent role in MN9D death. In order to investigate whether ULK1 implicated in MPP^+-induced MN9D death, we knocked down ULK1 expression using siRNA. The result showed ULK1 siRNA increased MN9D viability under MPP^+ treatment and demonstrated that ULK1 contributed to the MPP^+-induced MN9D death. Researchers have discovered that ULK1 could directly modulate mTORC1, the upstream Thr389 kinase of S6k1, and thereby negative regulated S6k1 [12]. To study whether ULK1 inhibited S6k1 phosphoryation, we determined the phosphorylation status of S6k1 after MPP^+ treatment. Our data showed that ULK1 knockdown enhance Sk61 phosphorylation especially at T389, whereas T421/s424 and S411 phosphorylation remained unaffected. Due to the negative effect of ULK1 on Sk61 phosphorylation under MPP^+ treatment, we desired to work out whether ULK1 block Sk61 phosphorylation at T389 in MN9D viability after MPP^+ treatment. The data reflected that phosphomimetic S6k1 T389D was obviously protective against MPP^+ toxicity; however, the phosphodeficient S6k1 T389A remark aggravate the MPP^+-induced cell death compared to the control. This data further confirmed the importance of Sk61 phosphorylation at T389 in maintaining MN9D viability.

In summary, the present study demonstrated that ULK1 inhibited phosphorylation of Sk61 at T389, contributing to neurodegeneration in the *in vitro* PD model. A better understanding of the role of ULK1 in PD will aid in improvement of PD treatment. Therefore, additional experiments *in vivo* will be needed to clarify the effect of ULK1 in PD in the future.

Authors' contributions

Yongle Li and Jun Zhang were responsible for the design and overall performance of the study as well as data analysis and preparation of the manuscript. Chunxiang Yang was involved in the design and conduct of this study. All authors read and approved the final manuscript.

Acknowledgments

None.

Transparency document

Transparency document related to this article can be found online at http://dx.doi.org/10.1016/j.bbrc.2015.02.008.

Conflicts of interest

None.

References

[1] I. Ferrer, Neuropathology and neurochemistry of nonmotor symptoms in Parkinson's disease, Parkinson's Dis. 2011 (2011) 1–13.
[2] C. Selman, J.M.A. Tullet, D. Wieser, E. Irvine, S.J. Lingard, A.I. Choudhury, et al., Ribosomal protein S6 kinase 1 signaling regulates mammalian life span, Science 326 (2009) 140–144.
[3] S.H. Um, D. D'Alessio, G. Thomas, Nutrient overload, insulin resistance, and ribosomal protein S6 kinase 1, S6K1, Cell Metab. 3 (2006) 393–402.
[4] Y. Xu, C. Liu, S. Chen, Y. Ye, M. Guo, Q. Ren, et al., Activation of AMPK and inactivation of Akt result in suppression of mTOR-mediated S6K1 and 4E-BP1 pathways leading to neuronal cell death in in vitro models of Parkinson's disease, Cell Signal 26 (2014) 1680–1689.
[5] Z. Hou, L. He, R.Z. Qi, Regulation of S6 kinase 1 activation by phosphorylation at Ser-411, J. Biol. Chem. 282 (2007) 6922–6928.
[6] M. Rosner, K. Schipany, M. Hengstschläger, p70 S6K1 nuclear localization depends on its mTOR-mediated phosphorylation at T389, but not on its kinase activity towards S6, Amino Acids 42 (2012) 2251–2256.
[7] Q. Zhou, C. Liu, W. Liu, H. Zhang, R. Zhang, J. Liu, et al., Rotenone induction of hydrogen peroxide inhibits mTOR-mediated S6K1 and 4E-BP1/eIF4E pathways, leading to neuronal apoptosis, Toxicol. Sci. 142 (2014) 1–16.
[8] Y. Chen, J. He, M. Tian, S.Y. Zhang, M.R. Guo, R. Kasimu, et al., UNC51-like kinase 1, autophagic regulator and cancer therapeutic target, Cell Proliferat. 47 (2014) 494–505.
[9] K. Maiese, Z.Z. Chong, Y.C. Shang, S. Wang, mTOR: on target for novel therapeutic strategies in the nervous system, Trends Mol. Med. 19 (2013) 51–60.
[10] S. Wang, J. Wu, S.-D. Nie, E. Bereczki, J.-J. Pei, Dysregulated mTOR-dependent signaling in neurodegeneration or carcinogenesis: implication for Alzheimer's disease and brain tumors, J. Alzheimer's Dis. 37 (2013) 495–505.
[11] S.B. Lee, S. Kim, J. Lee, J. Park, G. Lee, Y. Kim, et al., ATG1, an autophagy regulator, inhibits cell growth by negatively regulating S6 kinase, EMBO Rep. 8 (2007) 360–365.
[12] E.A. Dunlop, D.K. Hunt, H.A. Acosta-Jaquez, D.C. Fingar, A.R. Tee, ULK1 inhibits mTORC1 signaling, promotes multisite raptor phosphorylation and hinders substrate binding, Autophagy 7 (2011) 737.
[13] S. Przedborski, V. Jackson-Lewis, A.B. Naini, M. Jakowec, G. Petzinger, R. Miller, et al., The parkinsonian toxin 1-methyl-4-phenyl-1,2,3,6-tetrahydropyridine (MPTP): a technical review of its utility and safety, J. Neurochem. 76 (2001) 1265–1274.
[14] A.J. Linsenbardt, J.M. Breckenridge, G.H. Wilken, H. Macarthur, Dopaminochrome induces caspase-independent apoptosis in the mesencephalic cell line, MN9D, J. Neurochem. 122 (2012) 175–184.
[15] Y. Zhu, C. Wang, M. Yu, J. Cui, L. Liu, Z. Xu, ULK1 and JNK are involved in mitophagy incurred by LRRK2 G2019S expression, Protein Cell 4 (2013) 711–721.
[16] R.C. Scott, G. Juhász, T.P. Neufeld, Direct induction of autophagy by Atg1 inhibits cell growth and induces apoptotic cell death, Curr. Biol. 17 (2007) 1–11.
[17] N. Kanagaraj, H. Beiping, S.T. Dheen, S.S.W. Tay, Downregulation of miR-124 in MPTP-treated mouse model of Parkinson's disease and MPP iodide-treated MN9D cells modulates the expression of the calpain/cdk5 pathway proteins, Neuroscience 272 (2014) 167–179.
[18] B. Spittau, X. Zhou, M. Ming, et al., IL6 Protects MN9D cells and midbrain dopaminergic neurons from MPP+-induced neurodegeneration, Neuromol. Med. 14 (2012) 317–327.
[19] S. Hong, B. Zhao, D.B. Lombard, D.C. Fingar, K. Inoki, Cross-talk between sirtuin and mammalian target of rapamycin complex 1 (mTORC1) signaling in the regulation of S6 kinase 1 (S6K1) phosphorylation, J. Biol. Chem. 289 (2014) 13132–13141.